Applied Ergonomics 96 (2021) 103494

Contents lists available at ScienceDirect

Applied Ergonomics

journal homepage: www.elsevier.com/locate/apergo

Neural and biomechanical tradeoffs associated with human-exoskeleton interactions

Yibo Zhu [a], Eric B. Weston [b,c], Ranjana K. Mehta [a,*], William S. Marras [b,c]

[a] Wm. Michael Barnes '64 Department of Industrial & Systems Engineering, Texas A&M University, College Station, TX, 77840, USA
[b] Department of Integrated Systems Engineering, The Ohio State University, Columbus, OH, 43210, USA
[c] Spine Research Institute, The Ohio State University, Columbus, OH, 43210, USA

ARTICLE INFO

Keywords:
Spinal load
Brain activity
Human-robot interaction
Neuroergonomics
Manual handling

ABSTRACT

Industrial passive low-back exoskeletons have gained recent attention as ergonomic interventions to manual handling tasks. This research utilized a two-armed experimental approach (single vs dual-task paradigms) to quantify neural and biomechanical tradeoffs associated with short-term human-exoskeleton interaction (HEI) during asymmetrical lifting in twelve healthy adults balanced by gender. A dynamic, electromyography-assisted spine model was employed that indicated statistical, but marginal, biomechanical benefits of the tested exoskeleton, which diminished with the introduction of the cognitive dual-task. Using Near Infrared Spectroscopy (fNIRS)-based brain connectivity analyses, we found that the tested exoskeleton imposed greater neurocognitive and motor adaptation efforts by engaging action monitoring and error processing brain networks. Collectively, these findings indicate that a wearer's biomechanical response to increased cognitive demands in the workplace may offset the mechanical advantages of exoskeletons. We also demonstrate the utility of ambulatory fNIRS to capture the neural cost of HEI without the need for elaborate dual-task manipulations.

1. Introduction

Approximately 40% of work-related musculoskeletal disorder (WMSD) cases are low back injuries that account for more than 800,000 lost work days in 2019 and affect at least 50% of the working population in the United States (BLS, 2018, 2020). In the manufacturing industry, twisting and bending and frequent heavy lifting risks introduced by manual materials handling (MMH) tasks are major contributors to low back injuries, which costs more than $100 billion per year in US (Alterman et al., 2001). Robot-assisted ergonomic interventions, such as industrial exoskeletons, have shown promise in reducing WMSDs while maintaining productivity (De Looze, Bosch, Krause, Stadler, & O'Sullivan, 2016). However, some industrial exoskeletons may potentially exacerbate current WMSD risks in the workplace (NIOSH, 2018) by increasing muscle activity (Theurel et al., 2018), biomechanical loads on the lumbar spine (Weston et al., 2018), and metabolic cost (Gregorczyk et al., 2010), as well as introduce new risks, such as cognitive overload (Li et al., 2018).

An exoskeleton is defined as a wearable device that augments, enables, assists, or enhances wearer's motion, posture, or physical activity (ASTM, 2020). Exoskeletons can be categorized as active (powered) and passive (mechanical) to assist the user's motion and posture (Wesslén, 2018). Passive low-back exoskeletons have become more prevalent than active low-back exoskeletons when assisting MMH tasks, potentially due to their relatively low cost and ease of use (MacDougall, 2014). However, the evidence of the biomechanical benefits of exoskeletons remain mired in inconsistencies. For example, passive low-back exoskeletons have been found to provide limited biomechanical advantage during asymmetric MMH tasks, in terms of both trunk muscle activity and energy expenditure, than during symmetric MMH tasks (Alemi et al., 2020; Madinei et al., 2020). Several of these, and other, prior studies faced methodological inconsistencies; for example electromyographic (EMG) data was sometimes not normalized or modulated for muscle length and velocity relationships, kinematic data was often confined to just the sagittal plane or static assessments, or studies that used biomechanical models were often unable to account for the effect of muscle coactivity on tissue forces (Weston et al., 2018). Thus, studies employing biomechanical models that can accurately predict loads on the lumbar spine with and without exoskeleton use under complex lifting conditions (e.g., asymmetrical lifting) are still warranted. An understanding of lumbar

* Corresponding author. Industrial & Systems Engineering, Texas A&M University, College Station, TX, 77843, USA
.
E-mail address: rmehta@tamu.edu (R.K. Mehta).

https://doi.org/10.1016/j.apergo.2021.103494
Received 20 March 2021; Received in revised form 30 May 2021; Accepted 1 June 2021
Available online 11 June 2021

spinal loads relative to widely accepted tissue tolerance limits (Gallagher and Marras, 2012; Waters et al., 1993) is also expected to provide the most comprehensive picture of biomechanical risk for injury with and without an exoskeleton (Marras, 2012).

In addition to the lack of consensus regarding the effects of exoskeletons on biomechanical factors, it is evident that existing industrial exoskeleton designs emphasize physical fit while overlooking cognitive fit. Extraneous psychological and cognitive loading have been shown to increase spinal loads during MMH tasks (Marras and Hancock, 2014; Marras et al., 2000), further increasing the risk for a WMSD in the low back. Integrating physical and cognitive considerations in ergonomic interventions are thus warranted (Mehta, 2016). It is important that exoskeletons are designed and evaluated to ensure appropriate cognitive fit, such that the wearer has sufficient cognitive resources available to properly operate the exoskeleton as they conduct their daily work tasks (Stirling et al., 2020; Stirling et al., 2018). However, a few studies have examined the cognitive burden that exoskeletons place on its wearers (Bequette et al., 2020; Li et al., 2018; Maurice et al., 2019), and a recent study that has done so reported that an active exoskeleton demanded greater cognitive effort when compared to manually performing the task, which may lead to performance degradation and reduced effectiveness in preventing WMSDs (Stirling et al., 2018).

Methods used to evaluate the Human Exoskeleton Interaction (HEI) tend to vary widely and are each subject to their own list of limitations. The majority of cognitive fit assessment tools include usability tests and self-report surveys. However, these subjective measures can be biased and may lack reproducibility (Karwowski et al., 2003). Alternatively, another popular research method is to compare the changes in task performance or task-related muscle activity due to the introduction exoskeletons. These studies are limited, of course, in that they do not directly quantify neurocognitive effort, just what happens downstream. One option is to employ a dual task paradigm, in which subjects perform two tasks simultaneously to compare performance with a single-task condition. While the dual task performance approach is a worthy alternative to quantitatively measure cognitive load and attention level (Mehta and Parasuraman, 2013; Stirling et al., 2020), it is intrusive and may fundamentally alter user experience of the primary task (Mehta and Parasuraman, 2013; Parasuraman, 2011). Given the wide array of methods used and the limitations associated with each one, it is not surprising that previous results about the HEI are inconsistent. For example, a powered lower-body exoskeleton has been shown to impair user's reaction time in a dual task paradigm and increase user's mental workload through a self-report survey (Bequette et al., 2020). Conversely, in another investigation, passive low-back exoskeletons showed marginal improvements in precision task performance compared to the control (i.e., no exoskeleton) condition, quantified via measures trunk muscle activity, rating of perceived exertion, and task performance level (Madinei et al., 2020).

Over the past decades, the advent of modern neuroimaging techniques has allowed researchers to quantify neurocognitive effort directly based on brain-based metrics in human-robot applications across the transportation, aviation, and rehabilitation domains (Ayaz et al., 2012; Izzetoglu et al., 2011; Wismer et al., 2018). Different brain regions have their assigned roles for certain tasks or coordination of tasks, and for complex actions, multiple brain regions must work together to achieve task performance (Baker et al., 2018; Rhee and Mehta, 2018). In particular, HEI requires cooperative processing between and within the mind and motor pathways. For example, wearing a powered rehabilitation exoskeleton has shown to demand extra neural effort due to the human exoskeleton coupling, which requires greater neurocognitive processing and motor planning efforts (Federici et al., 2015; Meloni et al., 2011). Functionally meaningful correlations were first seen among primary motor cortex (M1), somatosensory (S1) regions during motor tasks (Vidoni et al., 2010). Dual tasking evoked activations in premotor cortex (PMC) and supplementary motor area (SMA) indicated active involvement of motor planning regions with increasing motor task complexity. On the other hand, interhemispheric functional connectivity strength within the dorsolateral prefrontal cortex (DLPFC) was also found to be positively correlated with mental workload levels (Causse et al., 2017; Fishburn et al., 2014; Vassena et al., 2019). Thus, it is important to understand brain dynamics, such as concurrent activation patterns and task-related connectivity, which measures task-related correlations among spatially different cortical regions (Friston, 2011), during HEI. Prior studies have also reported that initial HEI disrupts neuromuscular coordination (Gordon et al., 2013; Gregorczyk et al., 2010), is associated with increased motor complexity (Farris et al., 2013), and imposes greater cognitive demands (Bequette et al., 2020). It is thus likely that SMA, a key player in the action monitoring system (Desrochers et al., 2016), and medial prefrontal cortex (mPFC), engaged during error detection and processing (Bonini et al., 2014), may be functionally engaged during HEI. Therefore, task-related directed connectivity, which examines the influence that one brain region exerts over another (Friston, 2011), among DLPFC, PMC, and SMA may be useful markers in determining the nature and extent to which exoskeletons impact operators' neurocognitive and motor adaptation processes.

Finally, because exoskeletons have been designed primarily for physical fit, it is reasonable to assume that a trade-off exists between biomechanical and cognitive factors associated with their use. That is, a passive exoskeleton designed for the low back may reduce biomechanical loads on the lumbar spine at the cost of greater neurocognitive demands. The exact magnitude of this trade-off, however, is also important to quantify. If the exoskeleton increases cognitive demands so substantially that changes in muscle recruitment patterns, muscle coactivity, and subsequent increases in spinal loading occur, the biomechanical benefits of the exoskeletons itself might diminish or even disappear altogether. To the authors' knowledge, the biomechanical and cognitive impacts of HEI have yet to be investigated alongside one another in a formal laboratory study.

Therefore, the objective of this study was to concurrently quantify lumbar spinal loads and determine the neural signatures of HEI during a simulated MMH lifting task. To accomplish this objective, a two-study experimental approach was adopted. In Study 1, we first evaluated the effects of a passive low-back exoskeleton (i.e., condition) on biomechanical outcomes and connectivity changes between multiple brain regions of interests (ROIs) across two phases (early and late) during a 30-min asymmetrical lifting/lowering task. We hypothesized that in addition to motor regions, HEI will be associated with increased engagement of the cognitive control centers (e.g., mPFC) due to increased error mitigation effort when compared to manual unassisted lifting and that this cognitive adjustment would result in a change in the muscle recruitment patterns and subsequent spine tissue force. Study 2 was designed to further test this hypothesis by perturbing the cognitive regions of the brain via a cognitively demanding secondary dual task during a separate 30-min asymmetrical lifting/lowering task.

2. Methods

2.1. Participants

12 healthy and active adults (6 males, 6 females) with an activity history (self-reported) of at least 3 h per week of moderate intensity exercise for more than 3 months and no history of low back injuries were

Table 1
Study participant demographics and anthropometrics (Mean ± SD).

	Male	Female	Total
Number of Subjects	6	6	12
Age (years)	28.8 ± 4.8	24.6 ± 4.4	26.9 ± 4.7
Height (m)	1.790 ± 0.045	1.722 ± 0.046	1.759 ± 0.053
Weight (kg)	74.7 ± 12.2	59.5 ± 13.0	67.8 ± 11.6

recruited to participate in both studies. Demographic and anthropometric data (Mean ± SD) of the study participants are presented in Table 1. This study was approved by the Ohio State University Institutional Review Board [Approval ID: 2018H0569, Approval Date: 05/23/2019], and all participants signed informed consent forms before the experiment.

2.2. Experimental design

In each study, all participants were instructed to perform a simulated MMH task in two sessions on two separate days. One of the two sessions required the use of an exoskeleton, while the other did not. The sequence of two sessions was counterbalanced to prevent order and habituation effects.

Upon arrival to the laboratory for the first session, participants provided informed consent, and anthropometric measurements were obtained (stature, mass, width/depth of the torso at the xiphoid and umbilicus, circumference of the torso at the umbilicus) to scale the biomechanical spine model relative to that individual. During both sessions, subjects were outfitted with the necessary sensors (EMG, kinematic markers, fNIRS probe cap). The biomechanical spine model was calibrated to each individual according to a previously published calibration procedure (Dufour et al., 2013). If an exoskeleton was to be used for the session, it was fit to the subject according to the manufacturer's recommendations. Each participant was also given adequate time to familiarize themselves with the exoskeleton by bending over and squatting in it or practicing the experimental task for at least 5 min.

A 2 × 2 repeated measures design was implemented in this study, in which the effects of the exoskeleton condition (with and without the exoskeleton), phase (early 10 min and last 10 min work), and their interaction, were investigated for the Study 1 and 2 separately, detailed below.

2.2.1. Study 1: asymmetrical lifting/lowering

In this study, all participants transferred a 7.26 kg (16 lb.) medicine ball back and forth between an asymmetrical (45°) lift origin/destination at knee height and a symmetrical (0°) lift origin/destination at waist height without substantially moving their feet during each experimental task. Participants lifted and lowered using handles located on the opposite side of the medicine ball at a frequency of 6 lifts and lowers per minute for 30 min, paced by a digital metronome (Fig. 1, Matlab®, MA, USA). These specific conditions were selected based on our pilot work and previous MMH studies (Alemi et al., 2020; Antwi-Afari et al., 2017; Weston et al., 2020; Whitfield et al., 2014), to assure moderate physical demand levels and to minimize whole-body and localized muscle fatigue. Each participant conducted the lifting/lowering task with and without the exoskeleton on two different days randomly in order to explore the exoskeleton condition effect.

2.2.2. Study 2: asymmetrical lifting/lowering with a cognitive dual-task

Mental arithmetic is known to induce substantial psychological stress in laboratory settings (Allen and Crowell, 1989). In particular, a serial arithmetic subtraction task has previously been shown successfully induce cognitive overload during motor tasks (Schleifer et al., 2008). Therefore, to induce cognitive demand during the simulated MMH task in Study 2, all participants were instructed to follow the same physical asymmetrical lifting/lowering task protocol as described for Study 1 with a cognitively demanding secondary arithmetic subtraction task. Subjects were required to subtract 13 repeatedly from a random number between 500 and 1000 at the beginning of the task (Kase et al., 2009). Once the difference reached zero, participants were given a new random number for repeated subtraction. This process was repeated until the end of the 30-min physical cognitive task.

2.3. Instrumentation and apparatus

The tested passive exoskeleton was the Laevo™ V2.5 (Laevo, the Netherlands, Fig. 1). This exoskeleton consists of a chest pad and two leg pads that are connected by elastic beams. It harvests the kinetic energy during the lowering phase and restores the energy to aid user's motion during the lifting phase of the lift. Before the data collection, all participants were instrumented with the exoskeleton based on the manufacturer's guidelines and their comfort level.

Biomechanical loads in the lower back were measured using a validated EMG-assisted dynamic biomechanical spine model. This model's structure (Hwang et al., 2016) and validation for lifting tasks (Hwang et al., 2016) have been described previously. 10 wireless EMG sensors (Trigno™, Delsys, MA, USA) with sampling frequency of 1925.93 Hz were placed bilaterally on the trunk muscles, including the latissimus dorsi, erector spinae, rectus abdominis, internal oblique and external

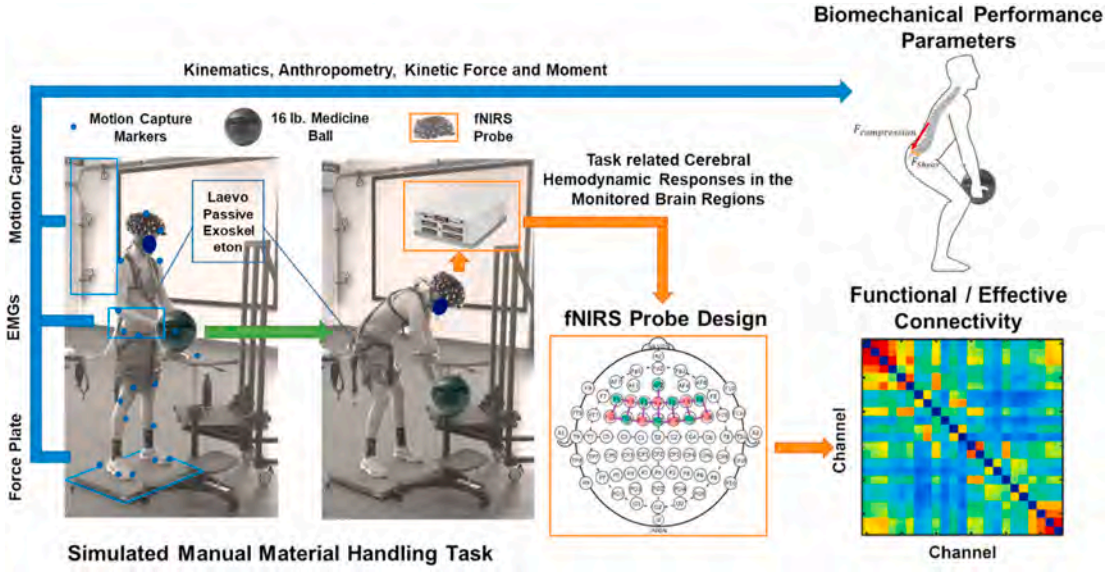

Fig. 1. Data collection, biomechanical and neuroergonomic feature extraction process during an exoskeleton-assisted MMH task. The spatial location of the 21-channel fNIRS Probe Design is presented following the international 10–20 system format (green and red dots indicate emitters and detectors respectively). (For interpretation of the references to color in this figure legend, the reader is referred to the Web version of this article.)

oblique according to standardized placement procedures (Mirka and Marras, 1993). Body segment kinematics were recorded via the OptiTrack Motion Capture System (NaturalPoint, OR, USA) with a sampling frequency of 120 Hz and processed in a customized laboratory software developed in Matlab (Mathworks, MA, USA). According to a kinematic model prescribed in the OptiTrack Motion Capture Software, 41 reflective optical motion capturing markers were placed over major body segments of each participant and 3 additional markers were fixed onto the force plate to track relative motion (Dufour et al., 2013). Kinetic force and moments data were sampled at a frequency of 1000 Hz using a FP6090-15 six-axial force plate (Bertec, OH, USA). Biomechanical data were synchronized using a USB-6225 data acquisition board (National Instruments, TX, USA).

Brain activation of each participant was monitored using a 20-channel portable continuous wave Functional near infrared spectroscopy (fNIRS) system, NIRSport2™ (NIRx Medical Technologies, NY, USA). fNIRS is an ambulatory system brain imaging technology which measures the neural activation related cerebral hemodynamic responses in task-related regions of the brain (Malonek and Grinvald, 1996). Its signal is relatively resilient to task related motion artifacts compared to the other commonly used brain imaging techniques, such as electroencephalogram (EEG) and functional magnetic resonance imaging (fMRI; Zhu et al., 2020). In the domain of human-robotic interaction, fNIRS has been applied to assess pilots' and surgeons' expertise levels as well as air traffic controllers' cognitive workload during simulated working tasks (Ayaz et al., 2012; Izzetoglu et al., 2011; Wismer et al., 2018). The NIRSport2 ™ system has 8 emitters and 8 detectors (Fig. 1). The inter-optode distance for each channel was set to be around 3 cm. During data collection, the sampling frequency of the device was set to 8.713 Hz. The light signals were emitted in two wavelengths (760 and 850 nm), and the probe was designed according to the clinically oriented anatomy-based Brodmann areas and their corresponding locations in the international 10–20 system format (Homan et al., 1987; Nolte, 1993). The center of the fNIRS cap was carefully aligned to the vertex (Cz) of each participant. In this configuration, six regions of interest (ROIs) were monitored, including the left, right, and medial dorsal lateral prefrontal cortex (lDLPFC, rDLPFC and mPFC), left/right premotor cortex (lPMC/rPMC), and supplementary motor area (SMA). To avoid signal contamination during the data collection, a black shower cap was worn by each participant on top of the fNIRS probe to block the infrared light emitted by the Motion Capture Cameras.

2.4. Data processing and analysis

2.4.1. Biomechanical analysis

EMG signals were first notch filtered at 60 Hz and band-pass filtered between 30 and 450 Hz. The filtered signals were then rectified, smoothed, and low-pass filtered using a zero-lag secondary-order Butterworth filter with a cut-off frequency of 1.59 Hz (selected from a time constant of 100 ms). Full body kinematic data were low-pass filtered using a fourth-order Butterworth filter with a cutoff frequency of 10 Hz. Based on the processed EMG signals, full body kinematic and kinetic data, Magnetic Resonance Imaging (MRI)-derived muscle locations and sizes, a multibody dynamic solver (Adams, MSC Software, Santa Ana, CA, USA) generated time-dependent spinal loads at the superior and inferior endplates of the lumbar spine extending from T12/L1 to L5/S1. Peak (i.e., maximum) loads along each dimension of spinal loading (compression at the L3/L4 Inferior endplate, anterior/posterior (A/P) shear at the L5/S1 Inferior endplate, lateral shear at the L5/S1 Superior endplate, resultant load at the L3/L4 vertebral level) were subsequently extracted for statistical analysis.

2.4.2. Neuroergonomic analysis

fNIRS signals were processed with the Homer2 software (Huppert et al., 2009). The light intensity signal acquired from each detector was first converted to optical density. The motion artifacts created by sudden movements from participants' head were corrected using spline interpolation (p = 0.99; Scholkmann et al., 2010) then smoothed using wavelet algorithm (kurtosis = 3.3; Chiarelli et al., 2015). The filtered signal was bandpass filtered at 0.015–0.5 Hz to reduce the physiological noise and signal drift (Zhu et al., 2020). In the end, the oxygenated (ΔHbO) and deoxygenated (ΔHbR) hemoglobin were calculated using the modified Beer-Lambert Law (Agbangla et al., 2017).

To identify potential phase effects, the calculated ΔHbO signals were separated into early (first 10 min of each experimental task) and late (last 10 min of each experimental task) phases. ΔHbO signal was chosen for further analysis, and it has previously show to better correlated with motor task-related brain activation compared to ΔHbR signal (Lu et al., 2010; Malonek and Grinvald, 1996).

Here, functional connectivity, which is computed on the basis of correlations among measurements of neural activation between different ROIs (Friston, 2011), were computed by calculating the Pearson correlations across all ROIs to find the correlations between ROIs. Pearson R values were then converted to fisher's z-scores to determine the strength of correlations (Rhee and Mehta, 2018). Two ROIs are considered functionally connected only when the corresponding Fisher's z-score equals or larger than to 0.4 (Rubinov and Sporns, 2010).

Time-domain effective connectivity analysis, which is examined as the time-dependent influence of one ROI on another (Friston, 2011), was conducted to identify any directed causal relationship among the cerebral hemodynamic responses (ΔHbO) in the monitored ROIs under each condition using the Multivariate Granger Causality toolbox (MVGC; Barnett and Seth, 2014; Friston, 2011). The autoregressive model, MVGC, is based on the concept of granger causality, a time-series variable X_B "causes" another time-series variable X_A if the past information of X_B improves the prediction of X_A better than only knowing the past of X_A (Granger, 1969). Assuming X_A and X_B are time-series signals of two ROIs, and they were fitted into two autoregressive models of order p:

$$X_A(t) = a_0 + \sum_{j=1}^{p} a_j X_A(t-j) + \varepsilon_A(t) \quad (1)$$

$$X_B(t) = b_0 + \sum_{j=1}^{p} b_j X_B(t-j) + \varepsilon_B(t) \quad (2)$$

Where the model order, p, represents the number of required past time-series values to predict the present values, and the residuals, $\varepsilon_A(t)$ and $\varepsilon_B(t)$, denote the prediction error of each model (Goebel et al., 2003). Each autoregressive model was then expanded to include their previous observations:

$$X_A(t) = a'_0 + \sum_{j=1}^{p} a'_j X_A(t-j) + \sum_{j=1}^{p} b'_j X_B(t-j) + \varepsilon_{BA}(t) \quad (3)$$

$$X_B(t) = b'_0 + \sum_{j=1}^{p} a'_j X_A(t-j) + \sum_{j=1}^{p} b'_j X_B(t-j) + \varepsilon_{AB}(t) \quad (4)$$

The granger causality magnitude, can be determined by comparing the variance of prediction errors through log-likelihood ratio:

$$F_{(B\to A)} = \ln\left(\frac{COV(\varepsilon_{BA})}{COV(\varepsilon_A)}\right) \quad (5)$$

$$F_{(A\to B)} = \ln\left(\frac{COV(\varepsilon_{AB})}{COV(\varepsilon_B)}\right) \quad (6)$$

In this study, the effective connectivity strength, quantified as the granger causality magnitude between any two ROIs, was calculated for each condition-phase combination across all participants.

2.5. Statistical analysis

Average values of the first 10 min (i.e., early phase) and the last 10

min (i.e., late phase) were computed for the biomechanical dependent variables, namely peak compression load at the L3/L4 Inferior endplate, peak A/P shear at the L5/S1 Inferior endplate, peak lateral shear at the L5/S1 Superior endplate, and resultant spinal load at the L3/L4 vertebral level. Additionally, functional and effective connectivity levels across ROIs were computed for the early and the late phases. All dependent variables were log-normalized where appropriate to meet parametric model assumptions. Separate two-way repeated measure analyses of variance (RANOVAs) were conducted to test the main effect of condition (control vs. exoskeleton), phase (early vs. late), and their interaction on the biomechanical performance parameters, namely peak spinal compression, A/P shear, lateral shear, and resultant spinal loads, as well as on functional and effective connectivity levels among ROIs. We conducted separate analyses for Study 1 and 2 to maximize results interpretability based on the study hypotheses. Results were analyzed using IBM SPSS Statistics (Version 23, Armonk, NY, USA). Statistical significance was tested relative to an alpha level of 0.05, and post-hoc analyses were conducted as needed using Bonferroni corrections. To reduce the likelihood of false positives caused by multiple comparisons for functional and effective connectivity analysis, the acquired p-values in each comparison were corrected using false discovery rate (FDR; with desired significance level of $q = 0.050$; Benjamini and Hochberg, 1995). Partial eta squared values were obtained as a measure of effect size.

3. Results

3.1. Study 1: asymmetrical lifting/lowering

3.1.1. Biomechanical analysis

No significant condition or condition × phase interaction effects were observed for L3/L4 Inferior Compression, L5/S1 Inferior Anterior Posterior Shear, or L3/L4 Resultant. However, peak lateral shear was found to be significantly higher in the control condition compared to the exoskeleton condition [$F(1,11) = 7.435$, $p = 0.021$, $\eta_p^2 = 0.426$; Table 2].

3.1.2. Functional connectivity analysis

A significant condition main effect was found on functional connectivity strengths between the following ROIs: left dorsal lateral prefrontal cortex (lDLPFC) - right premotor cortex (rPMC) [$F(1,11) = 7.891$, $p = 0.021$, $\eta_p^2 = 0.356$], medial prefrontal cortex (mPFC) - supplementary motor area (SMA) [$F(1,11) = 12.881$, $p = 0.005$, $\eta_p^2 = 0.563$], left premotor cortex (lPMC) - rPMC [$F(1,11) = 8.331$, $p = 0.016$, $\eta_p^2 = 0.454$], lPMC - SMA [$F(1,11) = 6.081$, $p = 0.033$, $\eta_p^2 = 0.378$], and rPMC - SMA [$F(1,11) = 7.733$, $p = 0.019$, $\eta_p^2 = 0.436$]. These identified connectivity strengths were all significantly higher in the exoskeleton condition than control (Fig. 2 top). Connectivity strength between lDLPFC and lPMC was significantly higher in the late phase compared to the early phase [$F(1,11) = 8.232$, $p = 0.017$, $\eta_p^2 = 0.452$] (Fig. 2 bottom). A marginally significant increase in connectivity strength between lDLPFC and rPMC was also found from early to late phase [$F(1,11) = 4.597$, $p = 0.058$, $\eta_p^2 = 0.223$]. Functional connectivity between rDLPFC and mPFC showed significant condition × phase interaction effect [$F(1,11) = 18.090$, $p = 0.020$, $\eta_p^2 = 0.644$]. Post hoc analysis showed the connectivity strength was significantly decreased in the late than the early phase in control but not in the exoskeleton condition ($p = 0.008$, Fig. 3).

3.1.3. Effective connectivity analysis

In order to further interpret the significant effects on functional connectivity changes, visual representations of significant effective connectivity among ROIs are shown in Fig. 4. In the early phase of the study, significant unidirectional effective connections from SMA to bilateral PMCs ($F = 0.012$, $p = 0.031$) and mPFC ($F = 0.011$, $p = 0.001$) regions were formed in the exoskeleton condition. Additionally, bidirectional effective connections between mPFC and lPMC ($F > 0.010$; $p < 0.001$) was also established. In the late phase of the study, unidirectional

Table 2
Biomechanical performance parameters (Mean SE) across the main and interactive effects of condition (control vs exoskeleton) and phase (early vs late) across study 1 and 2. * indicated statistical significance at $p < 0.05$.

Biomechanical Performance Parameters		Condition Main Effects	Phase Main Effect	Condition x Phase Effect
Study 1 (Physical Only Task)	L3/L4 Inferior Compression	Control: 2198.41 ± 133.49 N Exoskeleton: 2020.50 ± 134.15 N	Early: 2095.31 ± 120.73 N Late: 2123.60 ± 146.91 N	Control Early: 2133.52 ± 123.76 N Control Late: 2264.30 ± 143.23 N Exoskeleton Early: 2057.10 ± 117.71 N Exoskeleton Late: 1983.91 ± 150.58 N
	L5/S1 Inferior Anterior Posterior Shear	Control: 355.07 ± 22.91 N Exoskeleton: 320.50 ± 31.92 N	Early: 332.32 ± 22.43 N Late: 343.25 ± 32.39 N	Control Early: 343.29 ± 19.30 N Control Late: 366.85 ± 26.51 N Exoskeleton Early: 321.35 ± 25.57 N Exoskeleton Late: 319.66 ± 132.59 N
	L5/S1 Superior Lateral Shear	Control: 182.02 ± 51.08 N* Exoskeleton: 126.89 ± 42.70 N*	Early: 162.20 ± 42.79 N Late: 146.71 ± 47.78 N	Control Early: 189.11 ± 42.51 N Control Late: 174.92 ± 55.99 N Exoskeleton Early: 135.28 ± 43.08 N Exoskeleton Late: 118.49 ± 39.56 N
	L3/L4 Resultant	Control: 2203.41 ± 133.12 N Exoskeleton: 2025.14 ± 134.04 N	Early: 2100.21 ± 120.36 N Late: 2128.35 ± 146.80 N	Control Early: 2138.82 ± 123.25 N Control Late: 2268.00 ± 142.98 N Exoskeleton Early: 2061.59 ± 117.478 N Exoskeleton Late: 1988.70 ± 150.61 N
Study 2 (Physical Cognitive Dual-Task)	L3/L4 Inferior Compression	Control: 2217.18 ± 124.14 N Exoskeleton: 2255.05 ± 93.47 N	Early: 2191.25 ± 105.38 N* Late: 2289.98 ± 106.30 N*	Control Early: 2138.52 ± 127.29 N* Control Late: 2295.84 ± 134.12 N* Exoskeleton Early: 2243.98 ± 97.55 N Exoskeleton Late: 2266.11 ± 97.69 N
	L5/S1 Inferior Anterior Posterior Shear	Control: 386.35 ± 30.39 N Exoskeleton: 395.08 ± 39.85 N	Early: 387.34 ± 35.24 N Late: 394.10 ± 35.00 N	Control Early: 387.38 ± 27.24 N Control Late: 394.32 ± 33.54 N Exoskeleton Early: 396.29 ± 43.23 N Exoskeleton

(continued on next page)

Table 2 (*continued*)

Biomechanical Performance Parameters	Condition Main Effects	Phase Main Effect	Condition x Phase Effect
			Late: 393.88 ± 36.46 N
L5/S1 Superior Lateral Shear	Control: 192.48 ± 56.27 N Exoskeleton: 208.76 ± 55.31 N	Early: 194.58 ± 52.63 N Late: 206.66 ± 58.94 N	Control Early: 190.33 ± 51.66 N Control Late: 194.63 ± 60.87 N Exoskeleton Early: 198.84 ± 53.61 N Exoskeleton Late: 218.69 ± 57.01 N
L3/L4 Resultant	Control: 2223.13 ± 125.10 N Exoskeleton: 2263.07 ± 93.46 N	Early: 2198.01 ± 107.54 N Late: 2289.19 ± 111.03 N	Control Early: 2144.30 ± 121.86 N Control Late: 2301.97 ± 128.34 N Exoskeleton Early: 2251.72 ± 93.21 N Exoskeleton Late: 2274.43 ± 93.71 N

effective connections from SMA to bilateral PMCs ($F > 0.019$, $p < 0.032$) and lDLPFC ($F = 0.019$, $p = 0.031$) were observed in the exoskeleton condition. In general, SMA related causal density increased in the exoskeleton condition, when compared to the control condition, in both the early ($F_{control} = 0.005$; $F_{exoskeleton} = 0.010$) and late ($F_{control} = 0.005$; $F_{exoskeleton} = 0.011$) phases. mPFC related causal density was also higher in the exoskeleton condition compared to the control condition in both phases (early: $F_{control} = 0.006$; $F_{exoskeleton} = 0.007$; late: $F_{control} = 0.006$; $F_{exoskeleton} = 0.010$).

3.2. Study 2: asymmetrical lifting/lowering with a cognitive dual-task

3.2.1. Biomechanical analysis

No significant main effect of condition was observed for L5/S1 Inferior Anterior Posterior Shear (Mean = 390.72 N; SE = 35.12 N), and L5/S1 Superior Lateral Shear (Mean = 200.62 N; SE = 55.79 N) with all *p*-values greater than 0.459. A significant main effect of phase [$F(1,11) = 6.224$, $p = 0.032$, $\eta_p^2 = 0.384$] and a condition × phase interaction effect [$F(1,11) = 8.375$, $p = 0.016$, $\eta_p^2 = 0.446$] were found for peak L3/L4 Inferior compression (Table 2). Compressive forces were significantly higher in the late than the early phase (Table 2). Post hoc analysis revealed that this phase effect was only observed in the control condition and not the exoskeleton condition.

3.2.2. Functional connectivity analysis

Connectivity strength between rDLPFC and mPFC was significantly higher in the exoskeleton condition compared to the control condition (Fig. 5) [condition main effect: $F(1,11) = 16.871$, $p = 0.002$, $\eta_p^2 = 0.628$]. A significant condition × phase interaction effect was also observed [$F(1,11) = 6.726$, $p = 0.027$, $\eta_p^2 = 0.402$]. Connectivity strength between lDLPFC and SMA was found to be significantly higher in the exoskeleton condition than the control condition, however this was only observed in the late phase of the lifting/lowering task (Fig. 6).

3.2.3. Effective connectivity analysis

Significant effective connectivity paths are illustrated in Fig. 7. In the early phase, a unidirectional effective connection from SMA to mPFC

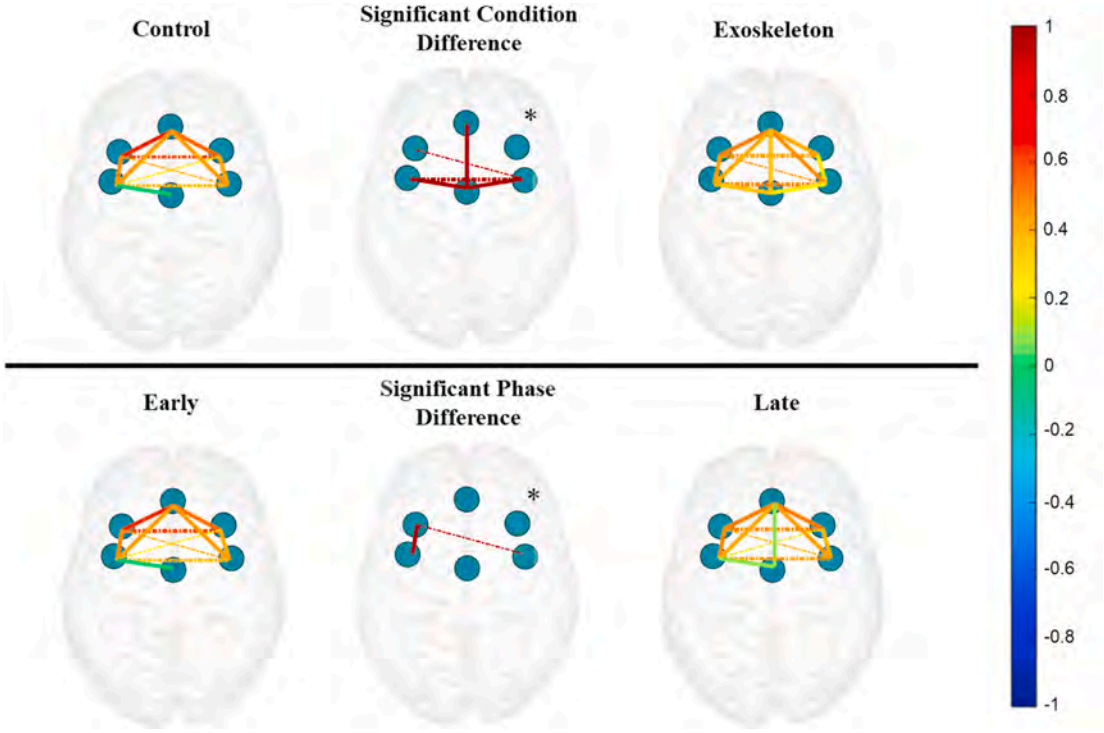

Fig. 2. Functional connectivity maps of study 1. Asterisk indicates functional connectivity strengths with significant condition main effect and significant phase main effect are shown in the top and bottom rows separately. The color of each line indicates the strength of functional connectivity based on the color scale on the right. Intra-hemispheric connections are represented by solid lines and inter-hemispheric connections are represented by dashed lines. Middle column shows significant changes between conditions and phases. All the lines in the middle column are in dark red (positive changes) which indicates significant stronger connectivity for the Exoskeleton condition than for the Control condition (top) and for the late than for the early phase (bottom). (For interpretation of the references to color in this figure legend, the reader is referred to the Web version of this article.)

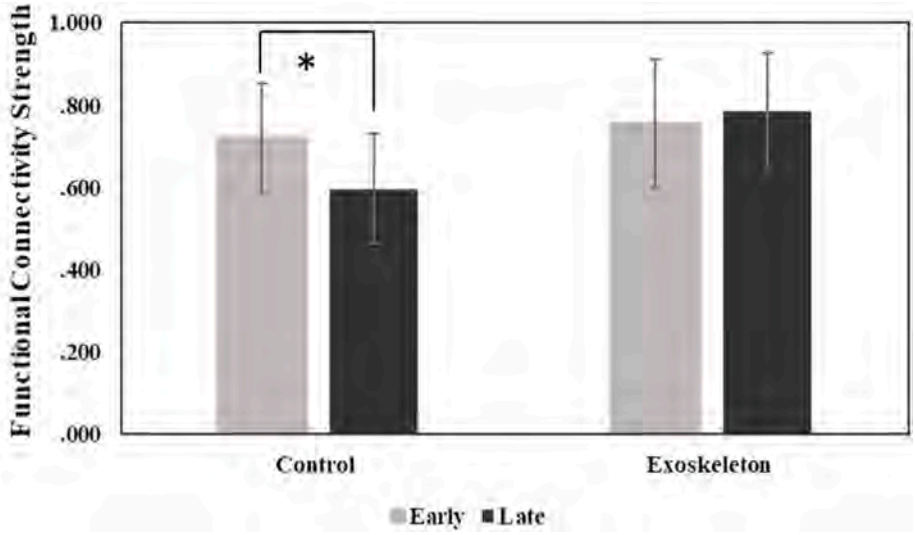

Fig. 3. Functional connectivity significant mixed effect of study 1. A significant condition × phase interaction effect between right dorsal lateral prefrontal cortex (rDLPFC) and medial prefrontal cortex (mPFC) functional connectivity strength (Mean ± SE) was observed; asterisk indicates significant decreases in functional connectivity over time in control condition but no such difference was seen in the exoskeleton condition.

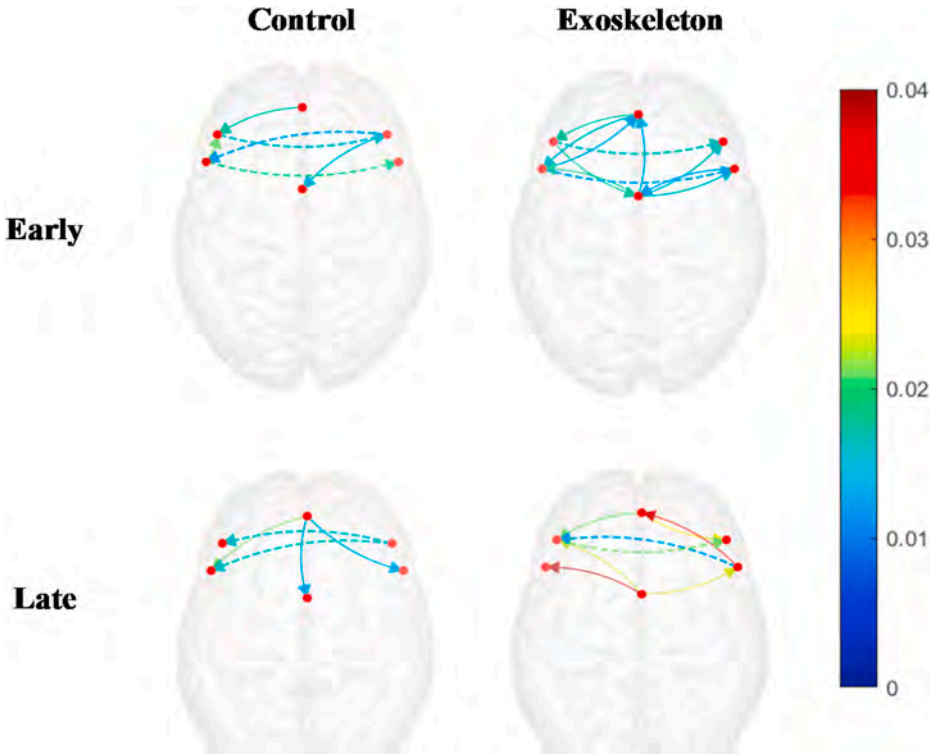

Fig. 4. Effective connectivity map of study 1. All effective connections shown are significant ($p < 0.05$). The color of each line indicates the strength of effective connectivity (granger causality) based on the color scale on the right. Solid lines indicate intra-hemispheric connections and dashed lines indicate inter-hemispheric connections. Multiple significant information flow paths were observed from supplementary motor area to premotor cortex (Early: $F = 0.012$, $p = 0.031$; Late $F < 0.019$, $p < 0.032$) and dorsolateral prefrontal cortex (Early: $F > 0.011$, $p < 0.012$; Late: $F = 0.019$, $p = 0.031$) regions in the exoskeleton condition. (For interpretation of the references to color in this figure legend, the reader is referred to the Web version of this article.)

region was formed in the exoskeleton condition ($F = 0.065$, $p < 0.001$). Additionally, mPFC was found to establish significant connections with all the other ROIs in the early phase exoskeleton condition ($p < 0.001$). In the late phase, both mPFC ($F > 0.013$, $p < 0.001$) and SMA ($F > 0.031$, $p < 0.001$) regions connected with rPMC region bidirectionally in the exoskeleton condition. Generally, SMA related causal density was greater in the exoskeleton condition in both the early ($F_{control} = 0.018$; $F_{exoskeleton} = 0.025$) and late ($F_{control} = 0.017$; $F_{exoskeleton} = 0.020$) phases compared to those in the control condition. Greater mPFC related causal density was also identified in the exoskeleton condition in both phases (early: $F_{control} = 0.013$; $F_{exoskeleton} = 0.022$; late: $F_{control} = 0.009$; $F_{exoskeleton} = 0.012$) than the control condition.

4. Discussion

To quantify the tradeoff that might exist between biomechanical measures (i.e., spinal loading) and neurocognitive effort with the use of a passive low-back assist exoskeleton, a two-armed experiment was conducted. In study 1, participants performed an asymmetrical lifting/lowering task with and without the exoskeleton. Wearing the exoskeleton reduced peak lateral shear forces acting on the lumbar spine but engaged operators' action monitoring system, as evidenced by increased fNIRS based functional connectivity and effective connectivity between supplementary motor area (SMA) and medial prefrontal cortex (mPFC) regions. In study 2, participants performed the same asymmetrical

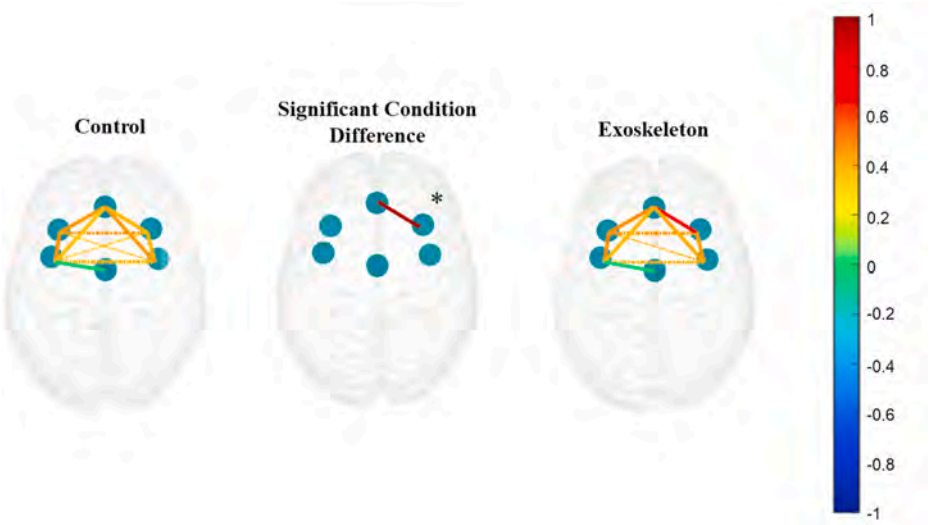

Fig. 5. Functional connectivity maps of study 2. Asterisk indicates a significant condition effect on the functional connectivity strength between right dorsal lateral prefrontal cortex (rDLPFC) and medial prefrontal cortex (mPFC). Six blue nodes in each graph indicate six regions of interest. The color of each line indicates the strength of functional connectivity based on the color scale on the right. Middle column shows significant changes between two conditions. The dark line (positive changes) in the middle column indicates significant stronger connectivity for the Exoskeleton Condition than for the Control Condition. (For interpretation of the references to color in this figure legend, the reader is referred to the Web version of this article.)

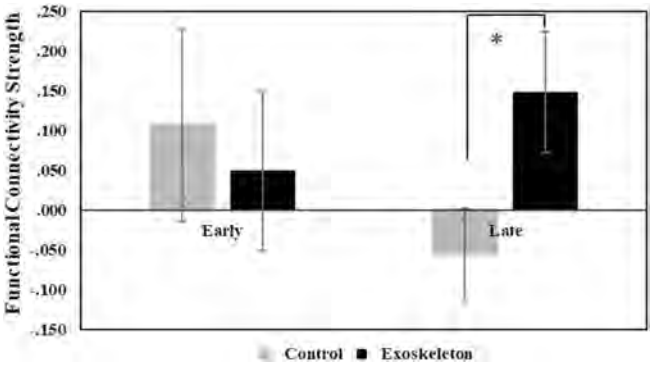

Fig. 6. Functional connectivity significant mixed effect of study 2. Study 2 yielded a significant condition × phase interaction effect between left dorsal lateral prefrontal cortex (lDLPFC) and supplementary motor area (SMA) functional connectivity strength (Mean ± SE); asterisk indicates significant difference in functional connectivity between Control and Exoskeleton condition in late phase but no such difference was seen in early phase ($p = 0.027$).

lifting/lowering task with the addition of a cognitively demanding secondary task. The biomechanical benefits of the exoskeleton were diminished, and greater cognitive control requirements of the lifting motion were observed, as evidenced by the engagement of the frontal lobe. Finally, an exoskeleton related motor adaptation process was captured through the neural connectivity patterns across both studies.

Several previous studies evaluating the effectiveness of exoskeleton use (particularly the one that was tested herein) have reported beneficial results, including decreased truck muscle activity and net joint moments for the exoskeleton relative to a control condition for both manual precision, static holding, and symmetric MMH tasks (Koopman et al., 2019; Koopman et al., 2020; Madinei et al., 2020). Contrary to the results of these prior studies, peak spinal compression was comparable across both control and exoskeleton conditions in the present experiment. This discrepancy may at least partially be explained by the nature of the lifting/lowering task performed, namely its asymmetry. Multiple studies have reported that passive low-back exoskeletons are less effective in reducing trunk muscle activity for asymmetrical MMH tasks (Alemi et al., 2019; Alemi et al., 2020; Madinei et al., 2020). For example, Alemi et al. (2020) observed a smaller reduction (13–15%) in peak trunk muscle activities during asymmetric MMH tasks with an exoskeleton as compared to symmetric MMH tasks with an exoskeleton (17–24%), which is likely attributable to poor physical human-exoskeleton coupling and the hazardous nature of the asymmetrical tasks.

Nonetheless, although the lateral shear forces observed for both the control and exoskeleton conditions were well below biomechanical damage thresholds (3400 N for compression and 700 N for shear loadings during repetitive tasks; Gallagher and Marras, 2012), a minor yet statistically significant reduction in the magnitude of peak lumbar lateral shear forces (55 N or about 12 lbs.) was observed for the exoskeleton condition in study 1. These results suggest that the tested exoskeleton may offer marginal biomechanical benefit relative to the control condition, at least when cognitive demand is low. However, an important takeaway should also be that changes in cognitive loading (discussed further below) may alter the biomechanical results and therefore, alter the effectiveness of exoskeleton use. In particular, the small biomechanical benefit of the exoskeleton that was observed in study 1 (i.e., reduction in lateral shear) was eliminated altogether as cognitive demands were increased in study 2. Indeed, previous literature suggests that cognitive or psychological stressors can exacerbate internal biomechanical loading (Mehta et al., 2011; Mehta and Agnew, 2012), particularly during MMH tasks (Marras et al., 2000). It is expected that the mechanism responsible for changes in internal biomechanical loading was increased torso muscle coactivity, which subsequently also increased spinal loading. Our muscle force data (Fig. 8) confirms that more muscle coactivity was present during lifting/lowering with the cognitive dual-task (study 2) than during the simple lifting/lowering task (study 1), particularly in the internal and external obliques.

It should also be noted that the increases in muscle coactivity and spinal loading resulting from increased cognitive loading were both more drastic and more immediate for the exoskeleton condition than the control condition. For example, differences in peak spinal compression between study 1 and study 2 for the control condition were just 0.23% and 1.39% for early and late phases respectively, whereas differences in spinal compression between study 1 and study 2 for the exoskeleton condition were 9.1% and 14.2% for early and late phases (Table 2). Likewise, regarding timing, the effects of increased cognitive loading may have taken some time to "set in" for the control condition, whereas the effects were apparent immediately for the exoskeleton condition. This could help to explain why the cognitive dual-task paradigm resulted in a statistically significant effect of phase (early vs. late) on L3/L4 Inferior compression in the control condition but not the exoskeleton condition.

The scientific literature points to other instances in which active and passive exoskeletons have both previously been shown to impair user's

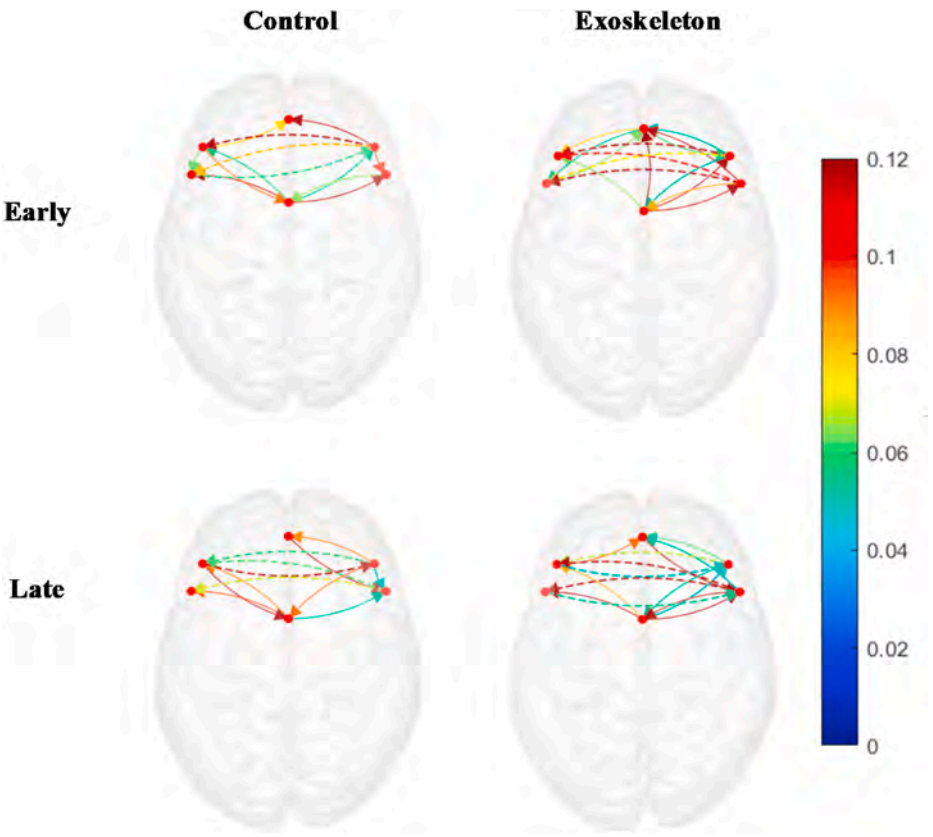

Fig. 7. Effective connectivity map of study 2. All effective connections shown are significant ($p < 0.001$). The color of each line indicates the strength of effective connectivity (granger causality) based on the color scale on the right. Solid lines indicate intra-hemispheric connections and dashed lines indicate inter-hemispheric connections. Significant information flow from supplementary motor area (SMA) to medial prefrontal cortex (mPFC) was observed only in the exoskeleton condition early phase ($F = 0.065$, $p < 0.001$) and diminished in the late phase. (For interpretation of the references to color in this figure legend, the reader is referred to the Web version of this article.)

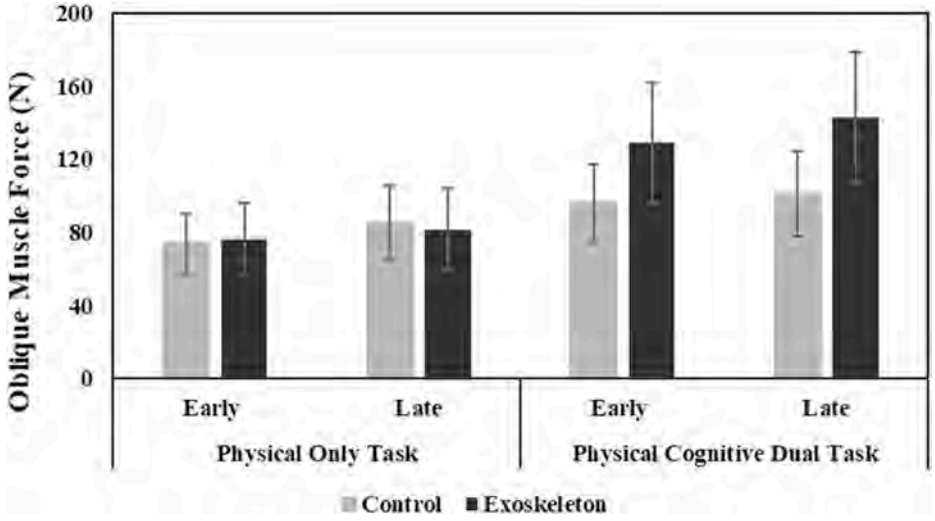

Fig. 8. External Oblique Muscle Forces (Mean ± SE). Greater muscle force was found during the physical cognitive dual-task (study 2) than the physical only task (study 1).

dual task performance and alter their working strategies (Bequette et al., 2018; Bequette et al., 2020; Federici et al., 2015; Meloni et al., 2011). However, while these studies support the notion that exoskeletons demand greater cognitive control of the physical task, they offer very little insight as to the mechanisms responsible for these findings. Moreover, by employing invasive cognitive dual-tasks, there is a risk associated with altering the very nature of the HEI. In the present study, we captured, for the first time, direct neural signatures of HEI during a movement-intensive MMH task. In general, compared to the no exoskeleton condition, lifting while wearing an exoskeleton required greater neural connectivity among the frontal (i.e., prefrontal cortex) and motor (i.e., premotor cortex, and supplementary motor area) regions (Fig. 2, top). Increased activation in the PFC is known to be positively correlated with working memory and complex cognitive processing (Harrison et al., 2014; McKendrick et al., 2017; Sibi et al., 2016). During complex motor tasks, the medial prefrontal cortex has shown to co-engage with supplementary motor area/premotor cortex regions and function as the central executive system to support motor planning and execution (D'Esposito, 2007; Nee & D'Esposito, 2016). As such, our results suggest that participants required greater cognitive control to regulate motor behavior during the MMH task in the exoskeleton condition (Tanaka and Kirino, 2017). We also observed that

the frontal brain regions remained functionally connected over time in the exoskeleton condition, while this connection disengaged in the control condition (Fig. 3). Because biomechanical benefits of the passive exoskeleton did not change over time (particularly in study 1), the tested exoskeleton required sustained engagement of the frontal regions. Additionally, stronger neural connectivity within the motor regions (i.e., supplementary motor area/premotor cortex) found in our study indicated that the HEI also required high-level motor control and planning than the control condition for the same physical task, thereby fundamentally changing the key characteristics (e.g., task complexity) of operator experiences as they performed the MMH tasks (Kim et al., 2018). Therefore, as hypothesized, our results highlighted that the tested passive low-back exoskeleton imposed greater cognitive processing, and motor planning demands to the operator during the simulated MMH task.

The hypothesis that HEI will involve the engagement of the frontal lobe, which is demonstrated by our study 1 findings, was further examined by perturbing the prefrontal cortex via a dual-task paradigm in study 2, similar to those adopted in prior studies (Beach et al., 2006; Davis et al., 2002; W. S. W. Marras et al., 2000). Here, we observed that the exoskeleton condition exhibited significantly greater connectivity strength between right dorsal lateral prefrontal cortex and medial prefrontal cortex regions (Fig. 5) than the control condition, suggesting that the cognitive dual-task had a greater impact on the frontal regions during HEI than during control, i.e., no exoskeleton, condition. This finding further validates our overarching hypothesis that HEI is associated with increased cognitive demands, evidenced by increased connectivity within prefrontal cortex regions (Causse et al., 2017; McKendrick et al., 2017; Vassena et al., 2019), and that the presence of any additional cognitive stressors (environmental or situational) will further neurocognitively burden operators wearing exoskeletons. More importantly, this effect was retained over time, thereby suggesting that HEI impact on neurocognitive effort during cognitively and physically demanding conditions remain elevated over time. Future longitudinal work is warranted that further investigates potential cognitive adaptation with HEI. We expected that similar to the neural patterns found in study 1, frontal and motor planning regions would remain engaged in the exoskeleton condition under dual-task in study 2, however, that was not the case here. It is likely that the connectivity strengths within the prefrontal cortex were much stronger than between prefrontal cortex and other motor regions, and thus these results dominated the statistical outcomes. This is supported by the magnitude of effect sizes observed here (greater than 0.6 for within prefrontal cortex and between 0.4 and 0.2 for between prefrontal cortex and supplementary motor area/-premotor cortex). Functional connectivity between the left dorsal lateral prefrontal cortex and supplementary motor area, however, increased significantly in the exoskeleton and decreased in the control condition over time (Fig. 6). It is likely that the added cognitive perturbation in the exoskeleton condition not only engaged more ROIs within the PFC than the physical MMH task, but over time expanded to co-engage supplementary motor area activation (i.e., the region regulating complex motor planning) to preserve task performance. Collectively, these results suggest that passive low-back exoskeletons may potentially reduce operators' cognitive resource availability and makes them vulnerable to extraneous and/or sudden cognitive perturbations (Stirling et al., 2018, 2020).

In general, HEI was also found to engage the action monitoring system in the cortex, which is typically responsible of action evaluation and error processing (Bonini et al., 2014). Featured by the causal connection from the supplementary motor area to the medial prefrontal cortex region, effective connectivity analyses revealed the recruitment of the SMA region to monitor the task performance, followed by the activation of the medial prefrontal cortex likely to process and correct motor coordination errors (Bonini et al., 2014; Seidler et al., 2013). For both study 1 and 2, such effective connectivity was observed only in the exoskeleton early phase which indicated that HEI was uncoordinated at the beginning of the MMH task. However, the effective connection from the supplementary motor area to the medial prefrontal cortex diminished in the late phases, implicating motor adaptation with HEI over time (Figs. 4 and 7).

There are some limitations that need to be acknowledged here. While the sample size is relatively small, it is comparable to existing ergonomic investigations on HEIs and include a balanced pool of men and women participants. More importantly, we observed large effect sizes (ranging from 0.2 to 0.6) and our major study hypothesis was confirmed. Second, limitations on the type of participants recruited (age group, sex, occupation) can impact the generalizability of the study findings and thus future work should expand to a broader range of participant demographics. In particular, formal evaluations of exoskeleton impacts on physical and cognitive demands in men and women are warranted. Third, our study inferences are limited to short-term evaluations of HEI that may be influenced by the intensity and pace of the simulated MMH tasks, which are on the lower end of physical demands when compared to other occupational biomechanics studies (Alemi et al., 2020; Madinei et al., 2020) or widely accepted lumbar biomechanical load limits (3400–6400 N compression, 700–1000 N shear; Gallagher and Marras, 2012; Waters et al., 1993). It is likely that the impact of HEI on physical or cognitive demand processing is a function of physical intensity levels (Mehta and Agnew, 2012), and thus future work that investigates how neural signatures change with more common physically demanding tasks under cognitive load (Grobe et al., 2017; Mehta, 2016) are warranted. In a similar vein, it is likely that different types of exoskeleton devices or models may impact operator cognitive-physical processing differently. As such, systematic neuroergonomic investigations that compare multiple exoskeleton devices and/or designs are needed that can set the foundation for evaluating different device features on their cognitive and motor processing requirements during various manual handling tasks.

Declaration of competing interest

The authors declare that they have no known competing financial interests or personal relationships that could have appeared to influence the work reported in this paper.

References

Agbangla, N.F., Audiffren, M., Albinet, C.T., 2017. Use of near-infrared spectroscopy in the investigation of brain activation during cognitive aging: a systematic review of an emerging area of research. Ageing Res. Rev. 38, 52–66. https://doi.org/10.1016/j.arr.2017.07.003.

Alemi, M.M., Geissinger, J., Simon, A.A., Chang, S.E., Asbeck, A.T., 2019. A passive exoskeleton reduces peak and mean EMG during symmetric and asymmetric lifting. J. Electromyogr. Kinesiol. 47, 25–34.

Alemi, M.M., Madinei, S., Kim, S., Srinivasan, D., Nussbaum, M.A., 2020. Effects of two passive back-support exoskeletons on muscle activity, energy expenditure, and subjective assessments during repetitive lifting. Hum. Factors 62 (3), 458–474.

Allen, M.T., Crowell, M.D., 1989. Patterns of autonomic response during laboratory stressors. Psychophysiology 26 (5), 603–614.

Alterman, T., Burnett, C., Lalich, N., MacDonald, L., 2001. A NIOSH look at data from the Bureau of Labor Statistics; worker health by industry and occupation: musculoskeletal disorders, anxiety disorders, dermatitis, hernia.

Antwi-Afari, M., Li, H., Edwards, D., Pärn, E., Seo, J., Wong, A., 2017. Biomechanical analysis of risk factors for work-related musculoskeletal disorders during repetitive lifting task in construction workers. Autom. ConStruct. 83, 41–47.

ASTM, 2020. Standard guide for quantitative measures for establishing exoskeleton functional ergonomic parameters and test metrics F48.02. Retrieved from. www.astm.org.

Ayaz, H., Çakir, M.P., İzzetoğlu, K., Curtin, A., Shewokis, P.A., Bunce, S.C., Onaral, B., 2012. Monitoring expertise development during simulated UAV piloting tasks using optical brain imaging. In: Paper Presented at the Aerospace Conference, vol. 2012. IEEE.

Baker, J.M., Bruno, J.L., Gundran, A., Hosseini, S.H., Reiss, A.L., 2018. fNIRS measurement of cortical activation and functional connectivity during a visuospatial working memory task. PloS One 13 (8), e0201486.

Barnett, L., Seth, A.K., 2014. The MVGC multivariate Granger causality toolbox: a new approach to Granger-causal inference. J. Neurosci. Methods 223, 50–68.

Beach, T.A., Coke, S.K., Callaghan, J.P., 2006. Upper body kinematic and low-back kinetic responses to precision placement challenges and cognitive distractions during repetitive lifting. Int. J. Ind. Ergon. 36 (7), 637–650.
Benjamini, Y., Hochberg, Y., 1995. Controlling the false discovery rate: a practical and powerful approach to multiple testing. J. Roy. Stat. Soc. B 57 (1), 289–300.
Bequette, B., Norton, A., Jones, E., Stirling, L., 2018. The effect of a powered lower-body exoskeleton on physical and cognitive warfighter performance. In: Paper Presented at the Proceedings of the Human Factors and Ergonomics Society Annual Meeting.
Bequette, B., Norton, A., Jones, E., Stirling, L., 2020. Physical and cognitive load effects due to a powered lower-body exoskeleton. Hum. Factors, 0018720820907450.
BLS, 2018. Back Injuries Prominent in Work-Related Musculoskeletal Disorder Cases in 2016. Bureau of Labor Statistics.
BLS, 2020. Employer-Reported Workplace Injuries and Illnesses. Bureau of Labor Statistics.
Bonini, F., Burle, B., Liégeois-Chauvel, C., Régis, J., Chauvel, P., Vidal, F., 2014. Action monitoring and medial frontal cortex: leading role of supplementary motor area. Science 343 (6173), 888–891.
Causse, M., Chua, Z., Peysakhovich, V., Del Campo, N., Matton, N., 2017. Mental workload and neural efficiency quantified in the prefrontal cortex using fNIRS. Sci. Rep. 7 (1), 5222.
Chiarelli, A.M., Maclin, E.L., Fabiani, M., Gratton, G., 2015. A kurtosis-based wavelet algorithm for motion artifact correction of fNIRS data. Neuroimage 112, 128–137. https://doi.org/10.1016/j.neuroimage.2015.02.057.
D'Esposito, M., 2007. From cognitive to neural models of working memory. Phil. Trans. Biol. Sci. 362 (1481), 761–772.
Davis, K.G., Marras, W.S., Heaney, C.A., Waters, T.R., Gupta, P., 2002. The impact of mental processing and pacing on spine loading: 2002 Volvo Award in biomechanics. Spine 27 (23), 2645–2653.
De Looze, M., Bosch, T., Krause, F., Stadler, K.S., O'Sullivan, L.W., 2016. Exoskeletons for industrial application and their potential effects on physical work load. Ergonomics 59 (5), 671–681.
Desrochers, T.M., Burk, D.C., Badre, D., Sheinberg, D.L., 2016. The monitoring and control of task sequences in human and non-human primates. Front. Syst. Neurosci. 9, 185.
Dufour, J.S., Marras, W.S., Knapik, G.G., 2013. An EMG-assisted model calibration technique that does not require MVCs. J. Electromyogr. Kinesiol. 23 (3), 608–613.
Farris, D.J., Robertson, B.D., Sawicki, G.S., 2013. Elastic ankle exoskeletons reduce soleus muscle force but not work in human hopping. J. Appl. Physiol. 115 (5), 579–585.
Federici, S., Meloni, F., Bracalenti, M., De Filippis, M.L., 2015. The effectiveness of powered, active lower limb exoskeletons in neurorehabilitation: a systematic review. NeuroRehabilitation 37 (3), 321–340.
Fishburn, F.A., Norr, M.E., Medvedev, A.V., Vaidya, C.J., 2014. Sensitivity of fNIRS to cognitive state and load. Front. Hum. Neurosci. 8, 76. https://doi.org/10.3389/fnhum.2014.00076.
Friston, K.J., 2011. Functional and effective connectivity: a review. Brain Connect. 1 (1), 13–36.
Gallagher, S., Marras, W.S., 2012. Tolerance of the lumbar spine to shear: a review and recommended exposure limits. Clin. BioMech. 27 (10), 973–978.
Goebel, R., Roebroeck, A., Kim, D.-S., Formisano, E., 2003. Investigating directed cortical interactions in time-resolved fMRI data using vector autoregressive modeling and Granger causality mapping. Magn. Reson. Imag. 21 (10), 1251–1261.
Gordon, K.E., Kinnaird, C.R., Ferris, D.P., 2013. Locomotor adaptation to a soleus EMG-controlled antagonistic exoskeleton. J. Neurophysiol. 109 (7), 1804–1814.
Granger, C.W., 1969. Investigating causal relations by econometric models and cross-spectral methods. Econometrica: Journal of the Econometric Society 424–438.
Gregorczyk, K.N., Hasselquist, L., Schiffman, J.M., Bensel, C.K., Obusek, J.P., Gutekunst, D.J., 2010. Effects of a lower-body exoskeleton device on metabolic cost and gait biomechanics during load carriage. Ergonomics 53 (10), 1263–1275.
Grobe, S., Kakar, R.S., Smith, M.L., Mehta, R., Baghurst, T., Boolani, A., 2017. Impact of cognitive fatigue on gait and sway among older adults: a literature review. Preventive medicine reports 6, 88–93.
Harrison, J., İzzetoğlu, K., Ayaz, H., Willems, B., Hah, S., Ahlstrom, U., Onaral, B., 2014. Cognitive workload and learning assessment during the implementation of a next-generation air traffic control technology using functional near-infrared spectroscopy. IEEE Transactions on Human-Machine Systems 44 (4), 429–440.
Homan, R.W., Herman, J., Purdy, P., 1987. Cerebral location of international 10–20 system electrode placement. Electroencephalogr. Clin. Neurophysiol. 66 (4), 376–382.
Huppert, T.J., Diamond, S.G., Franceschini, M.A., Boas, D.A., 2009. HomER: a review of time-series analysis methods for near-infrared spectroscopy of the brain. Appl. Opt. 48 (10), D280–D298.
Hwang, J., Knapik, G.G., Dufour, J.S., Aurand, A., Best, T.M., Khan, S.N., Marras, W.S., 2016a. A biologically-assisted curved muscle model of the lumbar spine: model structure. Clin. BioMech. 37, 53–59.
Hwang, J., Knapik, G.G., Dufour, J.S., Best, T.M., Khan, S.N., Mendel, E., Marras, W.S., 2016b. A biologically-assisted curved muscle model of the lumbar spine: model validation. Clin. BioMech. 37, 153–159.
Izzetoglu, K., Ayaz, H., Menda, J., Izzetoglu, M., Merzagora, A., Shewokis, P.A., Onaral, B., 2011. Applications of functional near infrared imaging: case study on UAV ground controller. In: Paper Presented at the International Conference on Foundations of Augmented Cognition.
Karwowski, W., Siemionow, W., Gielo-Perczak, K., 2003. Physical neuroergonomics: the human brain in control of physical work activities. Theor. Issues Ergon. Sci. 4 (1–2), 175–199.
Kase, S., Ritter, F., Schoelles, M.J., 2009. Serial subtraction errors revealed. In: Paper Presented at the Proceedings of the Annual Meeting of the Cognitive Science Society.
Kim, Y.K., Park, E., Lee, A., Im, C.-H., Kim, Y.-H., 2018. Changes in network connectivity during motor imagery and execution. PloS One 13 (1).
Koopman, A.S., Kingma, I., Faber, G.S., de Looze, M.P., van Dieën, J.H., 2019. Effects of a passive exoskeleton on the mechanical loading of the low back in static holding tasks. J. Biomech. 83, 97–103.
Koopman, A.S., Näf, M., Baltrusch, S.J., Kingma, I., Rodriguez-Guerrero, C., Babič, J., , . ., van Dieën, J.H., 2020. Biomechanical evaluation of a new passive back support exoskeleton. J. Biomech. 105, 109795.
Li, H., Cheng, W., Liu, F., Zhang, M., Wang, K., 2018. The effects on muscle activity and discomfort of varying load carriage with and without an augmentation exoskeleton. Appl. Sci. 8 (12), 2638.
Lu, C., Zhang, Y., Biswal, B.B., Zang, Y., Peng, D., Zhu, C., 2010. Use of fNIRS to assess resting state functional connectivity. J. Neurosci. Methods 186 (2), 242–249.
MacDougall, W., 2014. Industrie 4.0: smart manufacturing for the future. Germany Trade & Invest.
Madinei, S., Alemi, M.M., Kim, S., Srinivasan, D., Nussbaum, M.A., 2020. Biomechanical evaluation of passive back-support exoskeletons in a precision manual assembly Task:"Expected" effects on trunk muscle activity, perceived exertion, and task performance. Hum. Factors, 0018720819890966.
Malonek, D., Grinvald, A., 1996. Interactions between electrical activity and cortical microcirculation revealed by imaging spectroscopy: implications for functional brain mapping. Science 272 (5261), 551–554.
Marras, W., Allread, W., Burr, D., Fathallah, F., 2000. Prospective validation of a low-back disorder risk model and assessment of ergonomic interventions associated with manual materials handling tasks. Ergonomics 43 (11), 1866–1886.
Marras, W., Hancock, P., 2014. Putting mind and body back together: a human-systems approach to the integration of the physical and cognitive dimensions of task design and operations. Appl. Ergon. 45 (1), 55–60.
Marras, W.S., 2012. The complex spine: the multidimensional system of causal pathways for low-back disorders. Hum. Factors 54 (6), 881–889.
Marras, W.S., Davis, K.G., Heaney, C.A., Maronitis, A.B., Allread, W.G., 2000. The influence of psychosocial stress, gender, and personality on mechanical loading of the lumbar spine. Spine 25 (23), 3045–3054.
Maurice, P., Čamernik, J., Gorjan, D., Schirrmeister, B., Bornmann, J., Tagliapietra, L., Ivaldi, S., 2019. Objective and subjective effects of a passive exoskeleton on overhead work. IEEE Trans. Neural Syst. Rehabil. Eng. 28 (1), 152–164.
McKendrick, R., Mehta, R., Ayaz, H., Scheldrup, M., Parasuraman, R., 2017. Prefrontal hemodynamics of physical activity and environmental complexity during cognitive work. Hum. Factors 59 (1), 147–162.
Mehta, R.K., 2011. Interactive effects of physical and mental workload: a study of muscle function, capacity and exertion type. Virginia Tech.
Mehta, R.K., 2016a. Stunted PFC activity during neuromuscular control under stress with obesity. Eur. J. Appl. Physiol. 116 (2), 319–326.
Mehta, 2016b. Integrating physical and cognitive ergonomics. IIE Transactions on Occupational Ergonomics and Human Factors 4 (2–3), 83–87. https://doi.org/10.1080/21577323.2016.1207475.
Mehta, R.K., Agnew, M.J., 2012. Influence of mental workload on muscle endurance, fatigue, and recovery during intermittent static work. Eur. J. Appl. Physiol. 112 (8), 2891–2902.
Mehta, R.K., Parasuraman, R., 2013. Neuroergonomics: a review of applications to physical and cognitive work. Front. Hum. Neurosci. 7, 889. https://doi.org/10.3389/fnhum.2013.00889.
Meloni, F., Federici, S., Stella, A., 2011. The psychologist's role: a neglected presence in the assistive technology assessment process. Everyday technology for independence and care: AAATE 29, 1199–1206.
Mirka, G.A., Marras, W.S., 1993. Coactivation during trunk bending. Spine 18 (11), 1396–1409.
Nee, D.E., D'Esposito, M., 2016. The hierarchical organization of the lateral prefrontal cortex. Elife 5, e12112.
NIOSH, 2018. MSDs and emerging technologies (e.g. robots, exoskeletons).
Nolte, J., 1993. The Human Brain. Mosby/Elsevier.
Parasuraman, R., 2011. Neuroergonomics: brain, cognition, and performance at work. Curr. Dir. Psychol. Sci. 20 (3), 181–186.
Rhee, J., Mehta, R.K., 2018. Functional connectivity during handgrip motor fatigue in older adults is obesity and sex-specific. Front. Hum. Neurosci. 12.
Rubinov, M., Sporns, O., 2010. Complex network measures of brain connectivity: uses and interpretations. Neuroimage 52 (3), 1059–1069.
Schleifer, L.M., Spalding, T.W., Kerick, S.E., Cram, J.R., Ley, R., Hatfield, B.D., 2008. Mental stress and trapezius muscle activation under psychomotor challenge: a focus on EMG gaps during computer work. Psychophysiology 45 (3), 356–365.
Scholkmann, F., Spichtig, S., Muehlemann, T., Wolf, M., 2010. How to detect and reduce movement artifacts in near-infrared imaging using moving standard deviation and spline interpolation. Physiol. Meas. 31 (5), 649.
Seidler, R.D., Kwak, Y., Fling, B.W., Bernard, J.A., 2013. Neurocognitive mechanisms of error-based motor learning. In: Progress in Motor Control. Springer, pp. 39–60.
Sibi, S., Ayaz, H., Kuhns, D.P., Sirkin, D.M., Ju, W., 2016. Monitoring driver cognitive load using functional near infrared spectroscopy in partially autonomous cars. In: Paper Presented at the Intelligent Vehicles Symposium (IV), 2016 IEEE.
Stirling, L., , Kelty-Stephen, D., Fineman, R., Jones, M.L., Daniel Park, B.-K., Reed, M.P., Choi, H.J., 2020. Static, dynamic, and cognitive fit of exosystems for the human operator. Hum. Factors, 0018720819896898.
Stirling, L., Siu, H.C., Jones, E., Duda, K., 2018. Human factors considerations for enabling functional use of exosystems in operational environments. IEEE Systems Journal 13 (1), 1072–1083.

Tanaka, S., Kirino, E., 2017. Dynamic reconfiguration of the supplementary motor area network during imagined music performance. Front. Hum. Neurosci. 11, 606.
Theurel, J., Desbrosses, K., Roux, T., Savescu, A., 2018. Physiological consequences of using an upper limb exoskeleton during manual handling tasks. Appl. Ergon. 67, 211–217.
Vassena, E., Gerrits, R., Demanet, J., Verguts, T., Siugzdaite, R., 2019. Anticipation of a mentally effortful task recruits Dorsolateral Prefrontal Cortex: an fNIRS validation study. Neuropsychologia 123, 106–115.
Vidoni, E.D., Acerra, N.E., Dao, E., Meehan, S.K., Boyd, L.A., 2010. Role of the primary somatosensory cortex in motor learning: an rTMS study. Neurobiol. Learn. Mem. 93 (4), 532–539. https://doi.org/10.1016/j.nlm.2010.01.011.
Waters, T.R., Putz-Anderson, V., Garg, A., Fine, L.J., 1993. Revised NIOSH equation for the design and evaluation of manual lifting tasks. Ergonomics 36 (7), 749–776.
Wesslén, J., 2018. Exoskeleton exploration: research, development, and applicability of industrial exoskeletons in the automotive industry.
Weston, E.B., Alizadeh, M., Knapik, G.G., Wang, X., Marras, W.S., 2018. Biomechanical evaluation of exoskeleton use on loading of the lumbar spine. Appl. Ergon. 68, 101–108.
Weston, E.B., Aurand, A.M., Dufour, J.S., Knapik, G.G., Marras, W.S., 2020. One versus two-handed lifting and lowering: lumbar spine loads and recommended one-handed limits protecting the lower back. Ergonomics 1–17.
Whitfield, B.H., Costigan, P.A., Stevenson, J.M., Smallman, C.L., 2014. Effect of an on-body ergonomic aid on oxygen consumption during a repetitive lifting task. Int. J. Ind. Ergon. 44 (1), 39–44.
Wismer, A., Reinerman-Jones, L., Teo, G., Willis, S., McCracken, K., Hackett, M., 2018. A workload comparison during anatomical training with a physical or virtual model. In: Augmented Cognition: Users and Contexts, pp. 240–252.
Zhu, Y., Rodriguez-Paras, C., Rhee, J., Mehta, R.K., 2020. Methodological approaches and recommendations for functional near-infrared spectroscopy applications in HF/E research. Hum. Factors 62 (4), 613–642. https://doi.org/10.1177/0018720819845275.